Projections of Future Surface Air Temperature and Precipitation for the Middle Awash River Basins in Ethiopia using a Statistical Downscaling Model (SDSM)

Tesemash Abebe*

Department of Climate Science Research, Ethiopian Environment and Forest Research Institute, Addis A, Ethiopia

Corresponding Author*

Tesemash Abebe

Department of Climate Science Research, Ethiopian

Environment and Forest Research Institute, Addis A,

Ethiopia

E-mail: tese.leta@gmail.com

Received: 15-Jan-2023, Manuscript No. JCWF- 23-21584; **Editor assigned:** 17-Jan-2023, PreQC No. JCWF-23-21584 (PQ); **Reviewed:** 23-Jan-2023, QC No. JCWF- 23-21584 (Q); **Revised:** 28-Jan-2023, Manuscript No. JCWF- 23-21584 (R); **Published:** 31-Jan-2023, **DOI:** 10.35248/2332-2594.22.11(1).1-9

Abstract

In recent decades, climate change has become a major environmental and socioeconomic challenge in Ethiopia. The study used the statistically downscaled daily data in 30-year intervals from the second generation of the Earth System Model (CanESM2) under three Representative Concentration Pathways (RCPs): RCP2.6, 4.5, and 8.5 for three future time slices; near-term (2010-2039), mid-century (2040-2069), and end-century (2071-2099). The observed maximum and minimum temperature and precipitation values are a good simulation of the modeled data during the calibration and validation periods using the Pearson coefficient (R), the correlation coefficient (R2), and the Nash-Sutcliffe efficiency (NSE). In three sampled stations (Awash Arba, Shewa Robt, and Erer), there is a minor difference between all considered scenarios during the 2020s. The results of maximum and minimum temperature are expected to increase by 0.03°C–0.09°C and 0.05°C–0.2°C, respectively, during the 2020s. While the middle and far-future period's exhibit larger variations in the degrees of warming. The maximum and minimum temperature in the middle-future period (2050s) is likely expected to increase by 0.2°C–0.8°C and 0.2°C–1.93°C, respectively. During the 2080s, the worst-case scenarios (RCP8.5) are the ones with the greatest expected increase in maximum and minimum temperature of 1.03°C–1.6°C and 1°C–3.9°C, respectively, which are significantly higher than the remaining scenarios, varying approximately from 0.18°C–0.7°C and 0.13°C–1.6°C, respectively. In all the scenarios, the projected mean annual maximum and minimum temperature in the 2080s are the highest. The increment in minimum temperature is higher than the maximum temperature in almost all time slices under the three RCP scenarios. The mean annual precipitation is predicted to increase significantly at most stations over the three sampled stations in the middle Awash River basin. In the mid-future period (2050s), the mean annual precipitation will increase by 4.3%–16.4%. During the far-future period (2080s), the average annual precipitation is likely expected to increase by 3.4%–40.5% compared to the reference period. Temperature and precipitation are projected to increase in total amounts under all-time slices and emissions pathways. In all emission scenarios, the greatest changes in maximum temperature, minimum temperature, and precipitation are predicted by the end of the century. This implies that climate-smart actions in development policies and activities need to consider locally downscaling expected climatic changes.

Keywords: Statistical downscaling model • RCP scenarios • Climate change • General circulation model

Introduction

Climate change is already affecting every inhabited region across the globe, with human influence contributing many observed changes in weather and climate extremes. Global warming will continue, and addressing the challenges caused by climate change due to human influence has become a major issue of the 21st century [1]. Global surface temperature will continue to increase until at least mid-century under all emissions scenarios considered. Compared to 1850–1900, global surface temperature averaged over 2081–2100 is very likely to be higher by 1.0°C to 1.8°C under the very low GHG emissions scenario considered (SSP1- 1.9), by 2.1°C to 3.5°C in the intermediate GHG emissions scenario (SSP2- 4.5) and by 3.3°C to 5.7°C under the very high GHG emissions scenario (SSP5-8.5).24 The last time global surface temperature was sustained at or above 2.5°C higher than 1850–1900 was over 3 million years ago. Global warming of 1.5°C and 2°C will be exceeded during the 21st century unless deep reductions in CO_2 and other greenhouse gas emissions occur in the coming decades [1,2]. Additional global warming will very likely cause heavy precipitation events to intensify and become more frequent in most regions. At the global scale, extreme daily precipitation events are projected to intensify by about 7% for each 1°C of global warming [1]. Heavy precipitation and associated flooding are expected to intensify and become more common in most regions of Africa, Asia, North America, and Europe as global warming approaches 1.5°C [1].

The African continent has experienced increased warming since the beginning of the 20th century in regions where measurements allow a sufficient homogeneous observation coverage to estimate trends [3,4]. It is very likely that temperatures will increase in all future emissions scenarios and all regions of Africa. By the end of the century under RCP8.5, all African regions will very likely experience a warming larger than 3°C except Central Africa, where warming is very likely expected above 2.5°C, while under RCP2.6, the warming remains very likely limited to below 2oC. A very likely warming with ranges between 0.5°C and 2.5°C is projected by the mid-century for all scenarios depending on the region [3,4]. On other hand precipitation decreases in North Africa and West Southern Africa and medium confidence in East Southern Africa by the end of the 21st century[1,4,5]. The Western Africa region features a gradient in which precipitation decreases in the west and increases in the east and increase is also projected over Eastern Africa [6,7]. East Africa has experienced strong precipitation variability and intense wet spells leading to widespread pluvial flooding events hitting most countries including Ethiopia, Somalia, Kenya and Tanzania [8,9].

With the growing understanding of the physical processes underlying climate systems, Global Climate Models (GCMs) have become the primary tool and the most reliable sources for obtaining climate information over varied spatial and temporal scales [10,11]. However, GCMs have limited capacity to capture sub grid-scale features, not able to reliably provide regional- and local-scale projections due to their coarse resolution, and outputs from GCMs are still subject to biases [12]. They also have a finite capacity for studying hydrological processes and physical atmospheric processes at the regional scale [13,14]. Therefore, it is important to downscale GCM simulated climatic variables to local scales for use in impact assessment and adaptation planning. Downscaling is a widely used technique for bridging the gap between coarse GCM output and climate variable values at a finer resolution, and it can broadly be classified into dynamical and statistical downscaling techniques. Dynamical downscaling can be divided into two broad categories: one includes high-resolution Regional Climate Models (RCMs) with forced lateral boundary conditions from a host GCM; and another includes variable-resolution global models with local grid refinement over regions of interest, which are less common than RCMs but do not require lateral boundaries.In contrast, statistical downscaling is used to transform the outputs from GCMs to the local scale by establishing a statistical link between the local-scale meteorological series (predictand) and large-scale atmospheric variables. The dynamical approach is constrained by the availability of RCM simulations, and thus statistical downscaling techniques are more widely adopted due to their simplicity and low computational costs. In the last 20 years, a variety of statistical downscaling methods have been developed with a broad range of application in regional climate change studies. These methods can be classified by technique into regression methods, weather type approaches, and stochastic weather generators. Regression-based approaches have gained popularity out of the above three categories owing to their small requirement for computer resources and simplicity in realization, including multiple linear regression, generalized linear models, and machine learning

Journal of Climatology and Weather Forecasting 2023, Vol. 11, Issue 1, 001-09

techniques.

Materials and Methods

Description of the study area

The geographic location of the Awash River Basin is between 7°53'N and 12°N latitudes and 37°57'E and 43°25'E of longitudes. The total length of the river is about 1200 km and its catchment area is 113 700 km^2. The Awash River starts in the highlands of central Ethiopia near Ginchi town, in the west side of the capital city of Addis Ababa, at an altitude of about 3000 m above sea level and flows along the Rift Valley into the Afar Triangle, and terminates in the salty Lake Abbe on the border with Djibouti [15]. The Middle Awash River Basin (covering catchment area of approximately 20,000 km^2 out of whole basin 119,000 km^2) is located in apart of Great rift valley which is frequently affected by droughts[16]. It covers Oromia, Amhara and Afar regions [17]. The Awash River Basin is the most important basin in Ethiopia, and covers a total land area of 110,000 km^2 and serves as home to 10.5 million inhabitants [18,19]. The River rises on the high plateau, Ethiopia. The Koka Reservoir, about 75 km from Addis Ababa, has been in use since 1961 with a net available capacity of 1660 km^2 and a concrete dam that is 42 m high. The maximum rate of outflow through its turbines is 360 m^3 s^{-1}, and the normal annual outflow is about 120,000 m^3. Losses by evaporation are about 31,500 m^3 yr^{-1}, and by percolation about 38 000 m^3 yr^{-1}.

The climate of the Awash River Basin varies from humid subtropical over central Ethiopia to arid over the Afar lowlands [8]. There are three seasons in the Awash River Basin based on the movement of Inter Tropical Convergence Zone (ITCZ), the amount of rainfall and the rainfall timing. The three seasons are Kiremt, which is the main rainy season (June-September), Bega, which is the dry season (October-January), and Belg, the small rainy season (February-May) [20]. The mean annual rainfall varies from 1600 mm in the elevated areas to 160 mm in the lower Awash River Basin [21]. In the same way, the mean annual temperature of Awash River Basin ranges from 20.8°C in the middle part to 29°C in the lower part.

Data description

The station merged grid data of rainfall and temperature for Meddle Awash basin (Awash Arba, shewa Robt and Erer stations) was obtained from the Ethiopian National Meteorological institute (NMI) for the period of Jan/01/1983 to Dec/31/2016 and was used for model calibration and validation in SDSM. The baseline scenarios downscaled for base period for Awash Arba, shewa Robt and Erer stations using 33 years' daily data was selected to represent baseline. Thus, the CanESM2 was downscaled for the baseline period for the three RCPs scenarios and the statistical properties of the downscaled data were compared with observed data. Second Generation of Earth System Model (CanESM2): Developed at the Canadian Centre for Climate Modeling and Analysis (CCCma), this model consists of the physical coupled atmosphere-ocean model CanCM4 coupled to a terrestrial carbon model (CTEM) and an ocean carbon model (CMOC) [16]. CanESM2 provided CCCma's long term climate simulations for Phase 5 of the Coupled Model Inter-comparison Project, which in turn informed the Fifth Assessment Report (AR5) of the IntergovernmentalPanel on Climate Change [17].

Statistical Downscaling Model (SDSM)

The SDSM was introduced by Wilby and Dawson (2007) and a typical statistical downscaling tool that combines regression methods and a weather generator, and it has been widely applied in many fields [18,19]. It is well-recognized statistical downscaling tool which is applied widely in climate impact studies, was employed to transform the global circulation [6,20,21]. SDSM has been used to project future climate changes in many regions [22]. Furthermore, downscaling results based on SDSM are tuned by using bias correction so that the model can generate outputs closer to the observed data. Many bias-correction methods have been applied in statistical downscaling processes. Some take the mean and the variance into account; these methods include delta change, linear correction, nonlinear correction, and scaling correction [23]. Others take into consideration the probability distribution; these include, for instance, quantile mapping and some cumulative distribution function matching techniques [23].It is computationally inexpensive, able to directly incorporate the observational record of the region, etc. SDSM carried out seven key tasks including data quality control and transformation, screening variables, model calibration, frequency analyses, statistical analysis, scenario generation, and graphing of climate data to perform the downscaling and future projections [24,25] (Figure 1). The mathematical

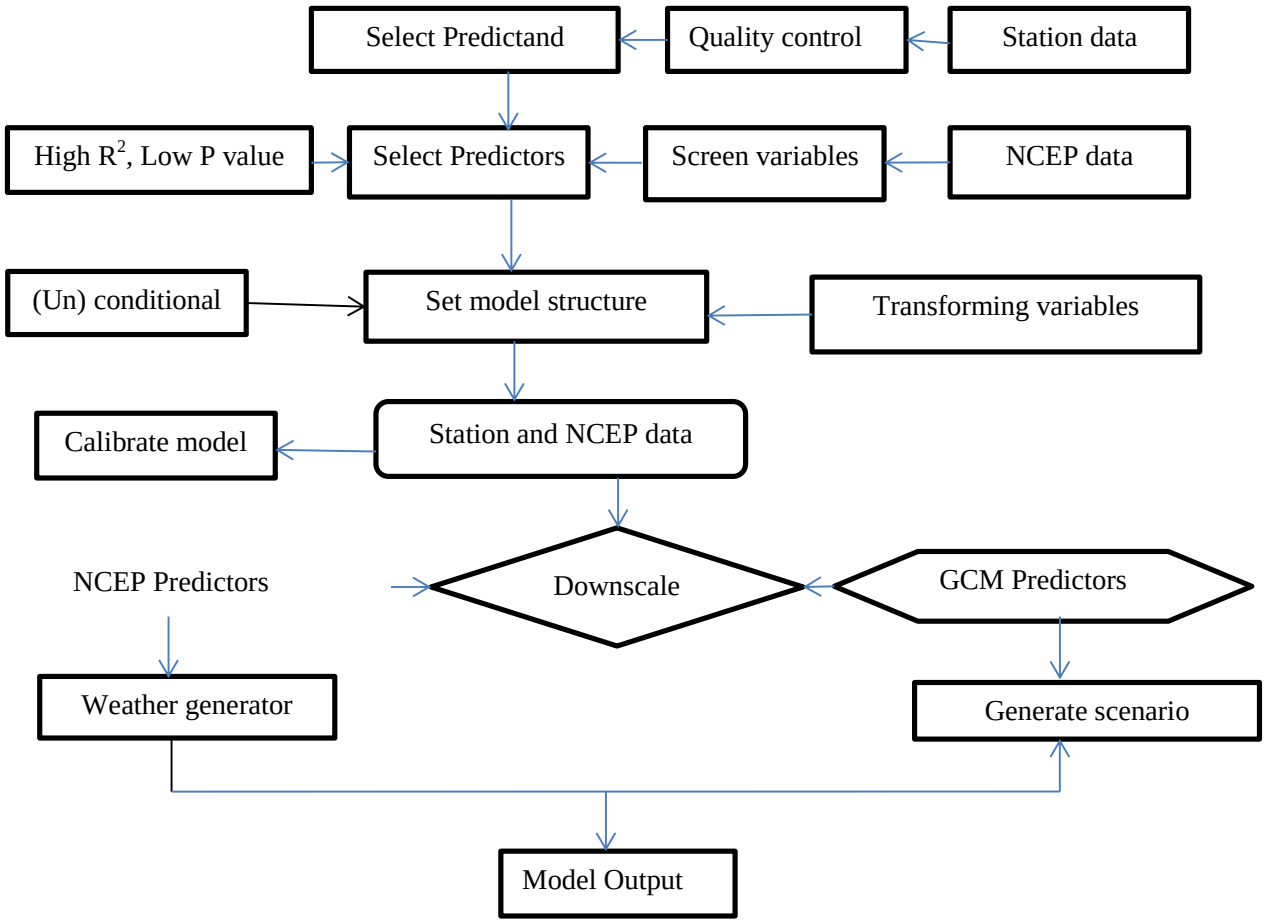

Figure 1. Steps involved in downscaling and scenario generation.

Journal of Climatology and Weather Forecasting 2023, Vol. 11, Issue 1, 001-09

details of this model are provided in the study by Wilby et al. 2014 [24]. The SDSM model contains two separate sub-models to determine the occurrence and amount of conditional meteorological variables (discrete variables), such as precipitation, and the number of unconditional variables (continuous variables), such as temperature or evaporation. Therefore, the SDSM can be classified as a conditional weather generator in which regression equations are used to estimate the parameters of daily precipitation occurrence and amount separately, making it slightly more sophisticated than a straightforward regression model [24]. Model calibration was done between 1983 and 2000, and model validation was done between 2001 and 2016. The calibrated model is used to generate future scenarios using the CanESM2 predictors available under RCP2.6, RCP4.5, and RCP8.5.

SDSM as the downscaling approach which required a proper selection of predictors established a relationship between predictors and predictand based on partial correlation coefficients. It is an important step in the downscaling process [6,25]. The predictors of the model were screened and selected based on the R2 and p-values. In order to have better prediction results, all the correlations with a p-value less than 0.05 were selected (Table 1).

The delta method is a simple, widely used method to create scenario time series from GCM output. The method uses the delta method of the SDSM for future projections [26,27]. The standard approach for the delta method is that the GCM-simulated difference for each calendar month (absolute difference for temperature and relative difference for precipitation) between a future period and the baseline period is determined and then this is superimposed on the historical daily temperature and precipitation series [28]. In the SDSM, a change in precipitation is obtained by:

$$\Delta 2020 = (\bar{U}2020s - \bar{U}base) \times 100)/\bar{U}base$$

The same is true for changes in 2050s and 2080s.

For the absolute value calculation (temperature in this case)

$$\Delta 2020s = \bar{U}2020 - \bar{U}base$$

The value at 2050s and 2080s is also obtained by the same formula explained in Equation (2).

$\bar{U}$ base is the mean of all ensembles (or a specific ensemble if selected) for each statistic for the baseline period. Likewise, $\bar{U}2020$ is the mean of all ensembles (a specific ensemble) for each statistic for period 2020s, and so on for $\bar{U}2050s$ and $\bar{U}2080s$ [25].

The Representative Concentration Pathway (RCPs)

RCPs are time- and space-dependent trajectories of future greenhouse gas concentrations and pollutants caused by human activities [29, 30]. It is the most recent set of time-dependent scenarios built on this two-decade development process. RCPs differ from earlier sets of standard situations by the radiative forcing projections, they are not emissions scenarios. The change in radiative forcing at the tropopause is connected to one value in each scenario [31, 32]. Each scenario is based on a single number: the difference in radiative forcing at the tropopause by 2100 compared to pre-industrial levels. The four RCPs are numbered 2.6 watts, 4.5 watts, 6.0 watts, and 8.5 watts per square meter (W/m^2), respectively, based on the change in radiative forcing by 2100 [29, 32]. This study focuses on the RCPs 2.6 (low), 4.5 (intermediate) and 8.5 (higher) scenarios. RCP2.6 emission and concentration pathway is representative of the literature on mitigation scenarios aiming to limit the increase of global mean temperature to 2°C. These scenarios form the low end of the scenario literature in terms of emissions and radiative forcing [33]. RCP4.5 includes the option of using policies to achieve net negative carbon dioxide emissions before the end of the century [34]. It is a scenario of long-term, global emissions of greenhouse gases, short-lived species, and land-use-land-cover which stabilizes radiative forcing at 4.5 W m^{-2} (approximately 650 ppm CO_2 equivalent) in the year 2100 without ever exceeding that value [35,36]. The RCP8.5 combines assumptions about high population and relatively slow income growth with modest rates of technological change and energy intensity improvements, leading in the long term to high energy demand and GHG emissions in absence of climate change policies [29,31,34,35]. Generally all RCP provides a common platform for climate models to explore the climate system response to stabilizing the anthropogenic components of radiative forcing.

Evaluation criteria

Due to examining the efficiency of the proposed downscale techniques, three evaluation criteria exist: Pearson coefficient (R), correlation coefficient (R2), and The Nash-Sutcliffe efficiency (NSE). R is the test statistics that measure the statistical relationship, or association, between two continuous variables. It gives information about the magnitude of the association, or correlation, as well as the direction of the relationship. The R2 value is typically employed as a measure of the degree of correlation between observed and simulated values. NSE shows how closely the line fits the plot of real versus simulated values. Higher R, R2 and NSE values are recommended for evaluation purposes [23,37,38]. The model generates up to 20 and more ensembles of daily time series using the identified best performing predictors, and its output is the mean of the ensembles and the ensembles were used for simulating each scenario for a period of 2020's 2050's and 2080's.

Results and Discussion

Calibration and validation

In this study, future climate scenarios were generated for T_{max}, T_{min} and precipitation by using SDSM 4.2 model at middle Awash River basin. The observed time series of temperature and precipitation were divided into two periods: the calibration period 1983–2000 and the validation period 2001-2016 for testing the model performance and comparing it with the downscaled results using the regression models (R, R2, and NSE).

Maximum temperature: During calibration the observed and simulated data, for three sample stations of Middle Awash basin R, R2, Nash models ranges between 0.85 up to 0.98 (Table 2). Each regression models (R, R2,

Table 1. List of predictors chosen for each climate variable.

Predictors	Awash Arba				Shewa Robt			Erer		
	Max. Temp	Min. Temp	Precip.		Max. Temp	Min. Temp	Precip.	Max. Temp	Min. Temp	Precip.
Mean sea level pressure							✓			
Surface airflow strength			✓							
Surface zonal velocity		✓			✓	✓	✓		✓	✓
Surface vorticity									✓	
Surface Wind Direction p1th		✓			✓	✓	✓		✓	
500 hPa vorticity								✓	✓	
500 hPa geopotential height	✓		✓		✓	✓	✓	✓		
500 hPa divergence	✓									
850 hPa airflow strength			✓							
850 hPa zonal velocity		✓		✓	✓	✓			✓	✓
850 hPa vorticity	✓							✓	✓	
850 hPa geopotential height		✓		✓		✓	✓	✓	✓	
850 hPa Wind Direction		✓		✓	✓	✓		✓		
850 hPa divergence	✓									
Specific humidity at 500 hPa		✓				✓				
Surface specific humidity					✓				✓	
Mean temperature at 2	✓	✓			✓	✓		✓	✓	

Journal of Climatology and Weather Forecasting 2023, Vol. 11, Issue 1, 001-09

and NSE) have a value very close to 1. However, as shown in Figure 1, the model overestimates the maximum temperature during the months of April, May and January in Awash Arba, May, July, August and November in Shewa Robt and June and November in Erer station A1, B1 and C1 (Figure 2). The validation results of sampled stations in each regression models showed good validation efficiency A2, B2 and C2 (Figure 2). In each case positive value close to 1 indicates good relation and high model efficiency in simulating the data by the model which is deployed for calibration and validation. The value greater than 0.5 is considered as good coefficient of determination and efficiency. In generally, the results of calibration and validation of maximum temperature in all stations indicates that there is very good agreement between observed and simulated maximum temperature.

Minimum temperature: During calibration the mean minimum temperature observed and simulated data for three sample stations of Middle Awash basin R, R2, Nash models ranges between 0.72 up to 0.97 (Table 2). Each regression models (R, R2, and NSE) have a value very close to 1. However, as shown in Figure 2, the model overestimates the minimum temperature during the months of June, September and October in Awash Arba, February, April and August in Shewa Robt and February, April and August in Erer station A1, B1 and C1 (Figure 3). The validation results of sampled stations in each regression models showed good validation efficiency A2, B2 and C2 (Figure 3). In each case positive value close to 1 indicates good relation and high model efficiency in simulating the data by the model which is deployed for calibration and validation. The value greater than 0.5 is considered as good coefficient of determination and

Table 2. Model performance evaluation.

Stations		Calibration			Validation		
	Climate elements	R	R2	NSE	R	R2	NSE
Awash Arba	Maximum Temperature	0.98	0.96	0.89	0.96	0.92	0.79
	Minimum Temperature	0.96	0.93	0.72	0.93	0.85	0.76
	precipitation	0.92	0.68	0.67	0.89	0.79	0.64
Shewa Robt	Maximum Temperature	0.93	0.87	0.85	0.92	0.84	0.83
	Minimum Temperature	0.97	0.87	0.88	0.96	0.92	0.85
	Precipitation	0.86	0.75	0.67	0.85	0.7	0.6
Erer	Maximum Temperature	0.92	0.93	0.92	0.92	0.93	0.92
	Minimum Temperature	0.91	0.93	0.91	0.85	0.92	0.85
	Precipitation	0.72	0.74	0.72	0.71	0.73	0.72

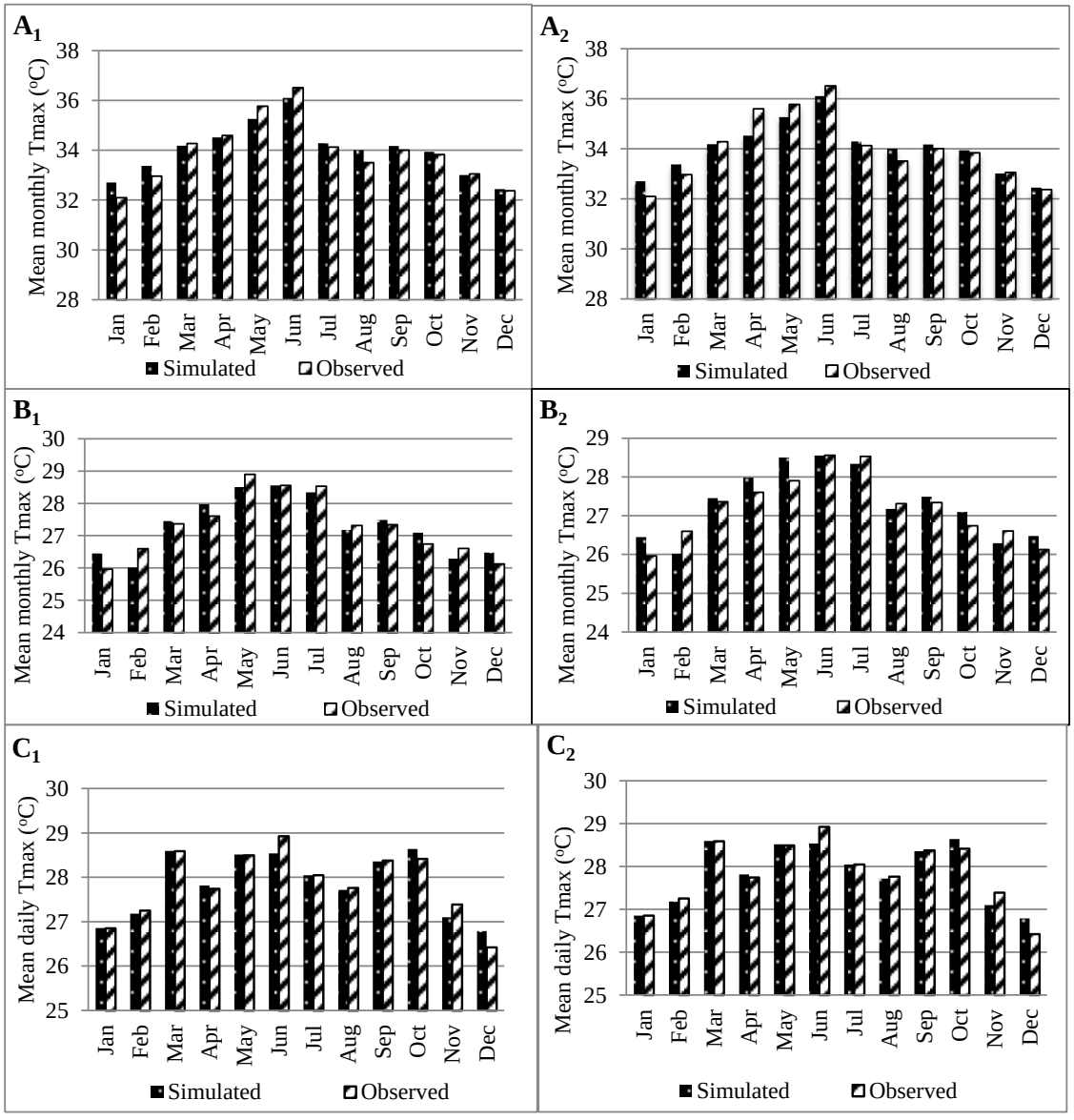

Figure 2. Calibration (A1, B1 and C1) and validation (A2, B2 and C2) results of mean monthly maximum temperature of Awash arba, Shewa robt and Erer stations

Journal of Climatology and Weather Forecasting 2023, Vol. 11, Issue 1, 001-09

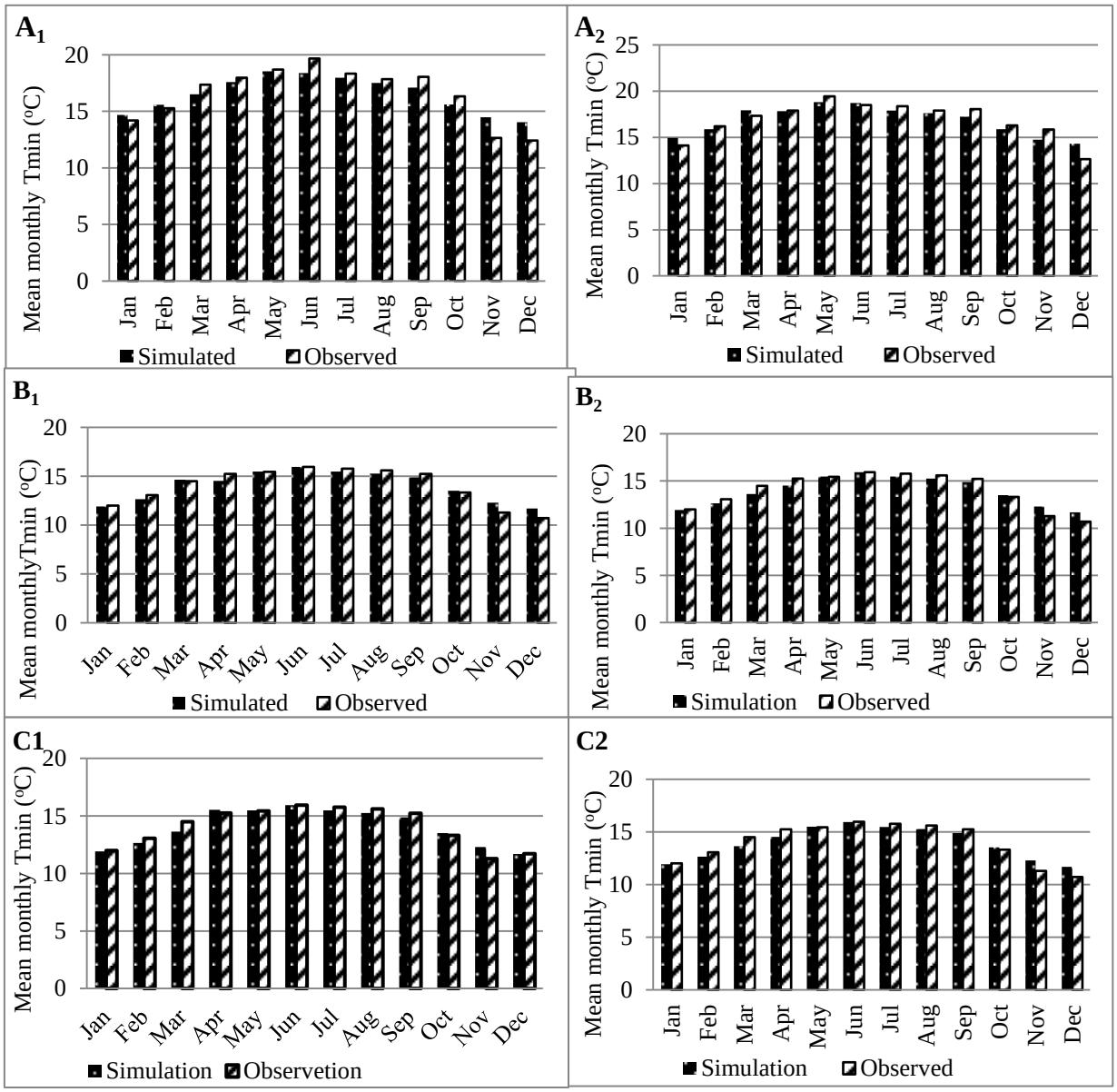

Figure 3. Calibration (A1, B1 and C1) and validation (A2, B2 and C2) results of mean monthly minimum of awash arba, shewa robt and erer stations

efficiency. In generally, the results of calibration and validation of minimum temperature in all stations indicates that there is very good agreement between observed and simulated minimum temperature.

Precipitation: During calibration the mean precipitation observed and simulated data for three sample stations of Middle Awash basin R, R2, Nash models ranges between 0.6 up to 0.92 (Table 2). Most of regression models (R, R2, and NSE) have a value less closed to 1 compared to maximum and minimum temperature. The possible reason for this the model structures of calibration can be category as the condition or un-condition process. By manual of SDSM 4.2, has stated that in conditional models a direct link is assumed between the predictors and predictand. In unconditional models, there is an intermediate process between the regional forcing and local weather e.g., local precipitation amounts depend on wet/dry-day occurrence, which in turn depend on regional-scale predictors (Figure 4). Therefore, predictand of temperature is set as un-condition and rainfall as the condition. Generally, the value of calibration and validation were greater than 0.5. So, the results of calibration and validation of mean precipitation were considered as good coefficient of determination and efficiency.

Future projection of middle awash basin

The study used the statistically downscaled daily data in 30-years intervals from the second generation of the Earth System Model (CanESM2) under RCPs 2.6, RCPs 4.5 and RCPs 8.5 for three future time slices; near-term (2010-2039), mid-century (2040-2069) and end-century (2071-2099) were generated.

Maximum and minimum temperature: The projected changes in annual average T_{max}, and T_{min} by calculating delta statistics (absolute difference) between the 2020s, 2050s, 2080s, and the reference period under CanESM2 RCP2.6, 4.5, 8.5 (Figures 5 and 6). The future T_{max} and T_{min} predictions results show that the increasing trend in all sampled stations. In all sampled stations there is a minor difference between all considered scenarios during the 2020s, while the middle and far-future periods exhibit larger variations in the degrees of warming. Particularly, T_{max} and T_{min} are predicted expected to increase by 0.03°C–0.09°C and are 0.05°C-0.2°C, respectively, during the 2020s compared to the reference period in all sampled stations.

Precipitation: Figure 6 shows in most sampled stations the annual

Journal of Climatology and Weather Forecasting 2023, Vol. 11, Issue 1, 001-09

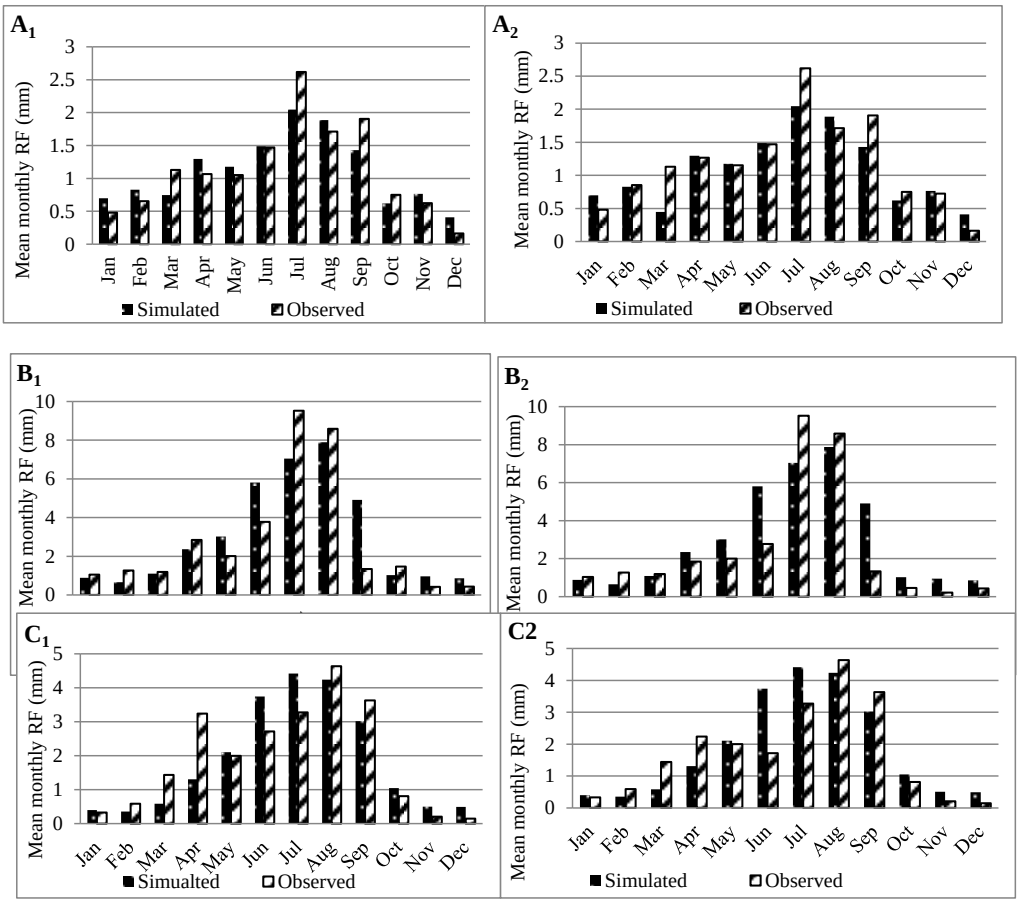

Figure 4. Calibration (A1, B1 and C1) and validation (A2, B2 and C2) results of mean monthly precipitation of Awash arba, Shewa robt and Erer stations.

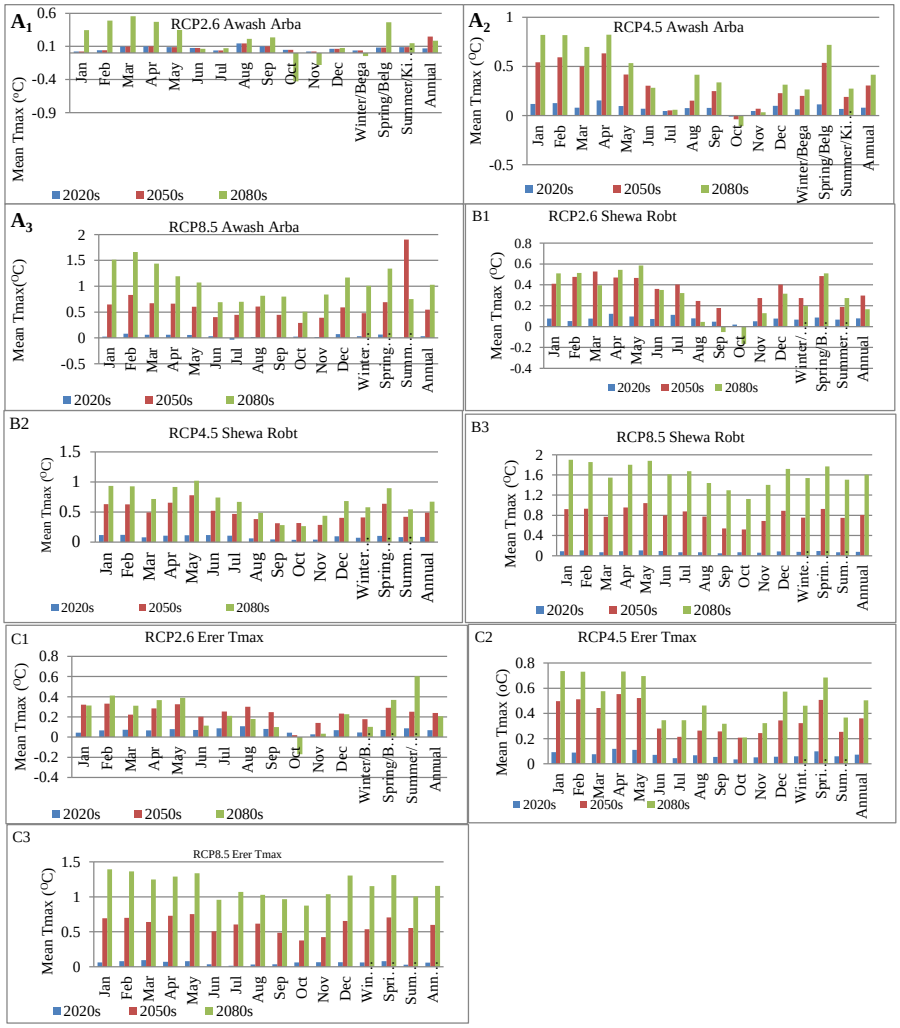

Figure 5. Projected changes in average annual maximum temperature in the 2020s, 2050s, and 2080s under scenarios RCP2.6, 4.5 and 8.5.

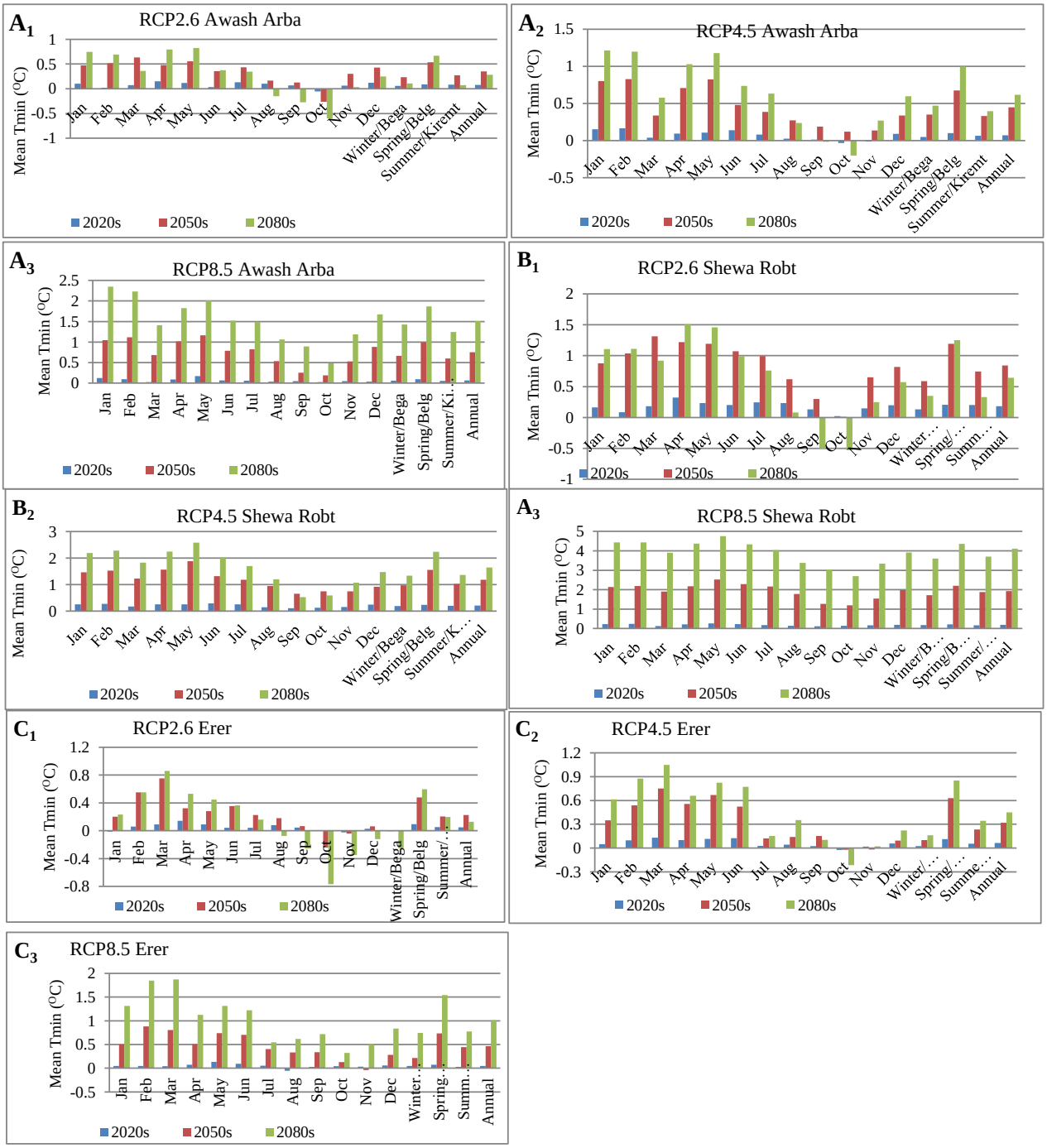

Figure 6. Projected changes in average annual minimum temperature in the 2020s, 2050s, and 2080s under scenarios RCP2.6, 4.5 and 8.5.

average precipitation is predicted to increase significantly at most stations over the middle Awash River basin. In the middle-future period (2050s), the annual average precipitation is increase by 4.3%–16.4%. During the far-future period (2080s), the average annual precipitation is likely expected to increase by 3.4%–40.5% compared to the reference period. However the results of Erer station shows expected to decreasing trend by -1, -3.3 in RCP2.6, the other scenario (RCP4.5 and 8.5) show increasing trend. A detailed description of projected changes in annual precipitation can be obtained from Figure 7.

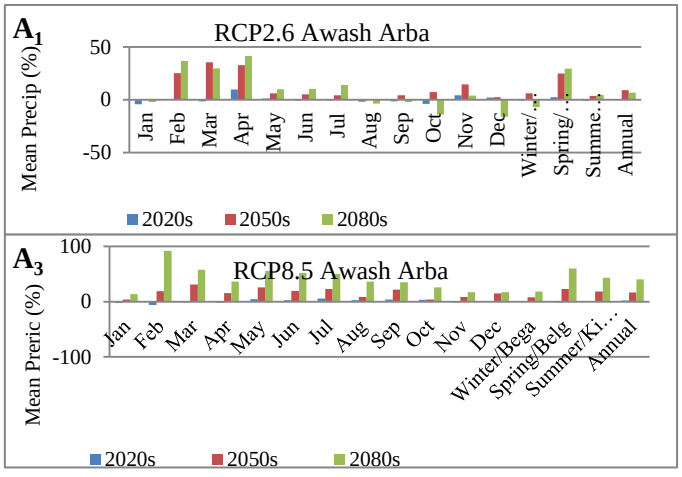

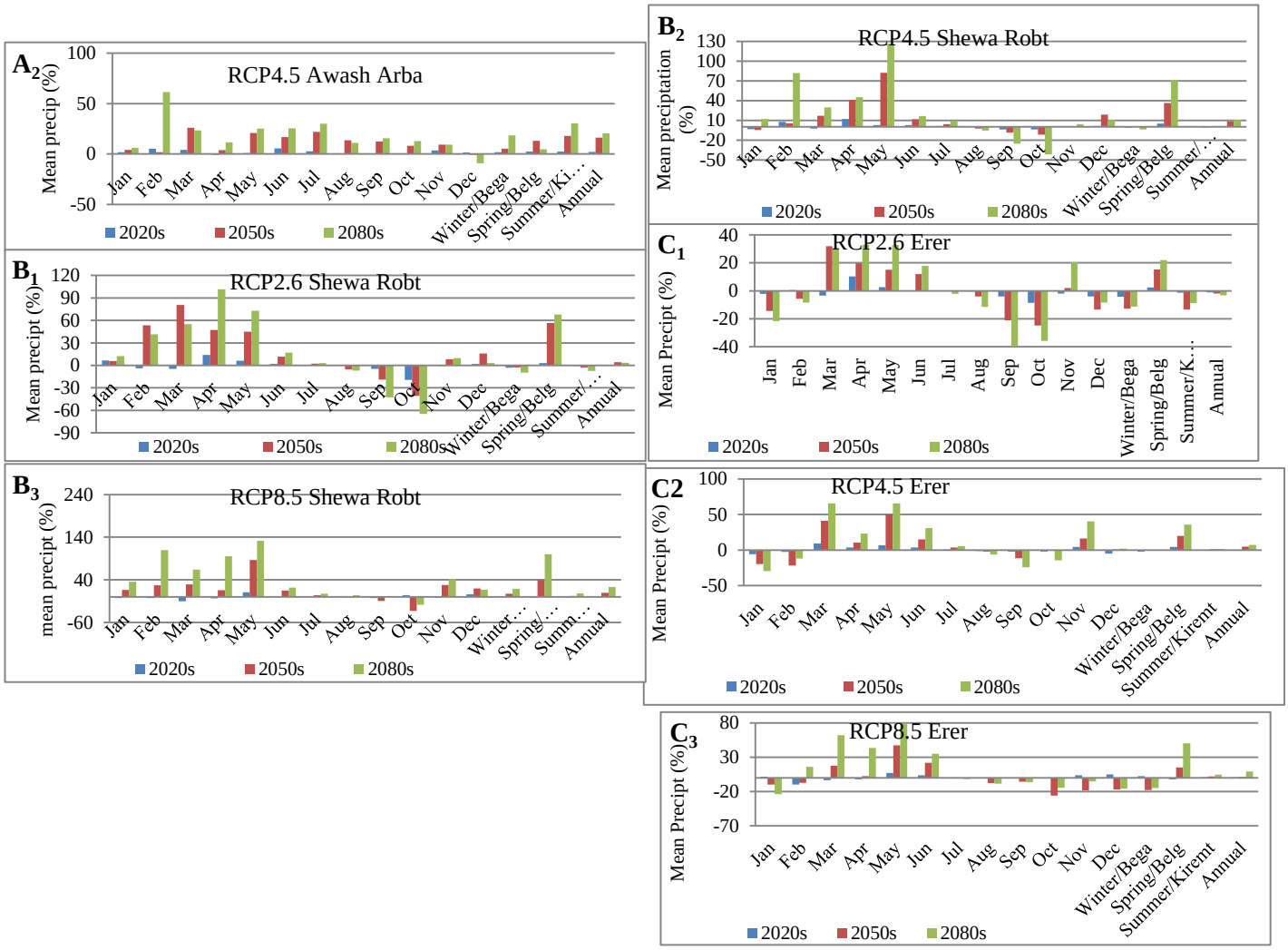

Figure 7. Projected changes in average annual precipitation in the 2020s, 2050s, and 2080s under scenarios RCP2.6, 4.5 and 8.5.

Summary and Conclusion

In this study, we applied a widely used statistical downscaling technique called SDSM for downscaling from large-scale variables to station-scale variables in the Middle Awash river basin. Then, the downscaled GCMs were used to project future temperature and rainfall changes over time and space under three different RCP scenarios.

The results of calibration the mean T_{max} observed and simulated data, for three sample stations of Middle Awash basin R, R2, Nash models ranges 0.85 to 0.98. The calibration of the mean T_{min} observed and simulated for three sample stations ranges from 0.72 to 0.97. Each regression model of T_{max} and T_{min} has a value very close to 1. However, the model overestimates the T_{max} during the months of April, May, and January in Awash Arba; May, July, August, and November in Shewa Robt; and June and November in Erer station. For T_{min}, the model overestimates during the months of June, September, and October in Awash Arba; February, April, and August in Shewa Robt; and February, April, and August in Erer station. The T_{max} and precipitation were considered to have a good coefficient of determination and efficiency.

All the downscaled projections under the three RCP scenarios show an increase in temperature with time, especially for RCP 8.5. In all sampled stations, there is a minor difference between all considered scenarios during the 2020s. The results of T_{max} and T_{min} are expected to increase by 0.03–0.09°C and 0.05°C–0.2°C, respectively, during the 2020s. While the middle and far-future period's exhibit larger variations in the degrees of warming. The T_{max} and T_{min} in the middle-future period (2050s) are likely expected to increase by 0.2°C–0.8°C and 0.2°C–1.93°C, respectively. During the 2080s, the worst-case scenarios (RCP 8.5) are the greatest expected to increase in T_{max} and T_{min} by 1.03°C–1.6°C and 1°C–3.9°C, which are significantly higher than the remaining scenarios varying approximately from 0.18°C –0.7 °C and 0.13°C–1.6°C, respectively. The increment in T_{min} is higher than the T_{max} in almost all time slices under the three RCP scenarios. In all the scenarios, the projected mean annual T_{max} and T_{min} in the 2080s are the highest. The mean annual precipitation is predicted to increase significantly at most stations over the middle Awash River basin. In the mid-future period 2050s, the mean annual precipitation will increase by 4.3%–16.4%. During the far-future period (2080s), the average annual precipitation is likely expected to increase by 3.4%–40.5% compared to the reference period. However, while the results of Erer Station show an expected decreasing trend of -1 to -3.3 in RCP2.6, the other scenarios (RCP4.5 and 8.5) show an increasing trend. This implies that climate-smart actions in development policies and activities need to consider locally downscaling expected climatic changes.

T_{min} validation results of all sampled stations in each regression model showed good validation efficiency. In each case, a positive value close to 1 indicates good relationships and high model efficiency in simulating the data by the model that is deployed for calibration and validation. In general, the results of the calibration and validation of T_{max} and T_{min} at all stations indicate that there is very good agreement between observed and simulated data. In the case of mean precipitation, the observed and simulated data for three sample stations R, R2, Nash models ranges from 0.6 to 0.92. Most of regression models have a value less closed to 1 compared to T_{max} and T_{min}. The possible reason for this model structure of calibration can be categorized as a conditional or unconditional process. By manual of SDSM 4.2, has stated that in conditional models a direct link is assumed between the predictors and predictand. In unconditional models, there is an intermediate process between the regional forcing and local weather e.g., local precipitation amounts depend on wet/dry-day occurrence, which in turn depend on regional-scale predictors. Therefore, predictand of temperature is set as un-condition and rainfall as the condition. Generally, the values of calibration and validation were greater than 0.5. So, the results of the calibration and validation of the mean

Journal of Climatology and Weather Forecasting 2023, Vol. 11, Issue 1, 001-09

References

1. Masson-Delmotte, et al. "Climate change 2021: the physical science basis." Contribution of working group I to the sixth assessment report of the intergovernmental panel on climate change 2 (2021).
2. Gebregeorgis, et al. "Historical droughts recorded in extended Juniperus procera ring-width chronologies from the Ethiopian Highlands." *International journal of biometeorology* 64 (2020): 739-753.
3. Ranasinghe, R, et al. "Climate change information for regional impact and for risk assessment." (2021): 1767-1926.
4. Kew, Sarah F., et al. "Impact of precipitation and increasing temperatures on drought trends in eastern Africa." *Earth System Dynamics* 12.1 (2021): 17-35..
5. Liu, Lan-Ya, et al. "Projections of surface air temperature and precipitation in the 21st century in the Qilian Mountains, Northwest China, using REMO in the CORDEX." *Advances in Climate Change Research* 13.3 (2022): 344-358.
6. Fan, et al. "Statistical downscaling and projection of future temperatures across the Loess Plateau, China." *Weather and Climate Extremes* 32 (2021): 100328.
7. Chen, et al. "Global land monsoon precipitation changes in CMIP6 projections." *Geophysical Research Letters* 47.14 (2020): e2019GL086902.
8. Haile, et al. "Long-term spatiotemporal variation of drought patterns over the Greater Horn of Africa." *Science of the Total Environment* 704 (2020): 135299.
9. Gebrechorkos, et al. "Changes in temperature and precipitation extremes in Ethiopia, Kenya, and Tanzania." *International Journal of Climatology* 39.1 (2019): 18-30. [GoogleScholar]
10. Eden, et al. "Downscaling of GCM-simulated precipitation using model output statistics." *Journal of Climate* 27.1 (2014): 312-324..
11. Sun, C. X., et al. "Drought occurring with hot extremes: Changes under future climate change on Loess Plateau, China." *Earth's Future* 7.6 (2019): 587-604.
12. Xu, L., et al. "Hot spots of climate extremes in the future." *Journal of Geophysical Research: Atmospheres* 124.6 (2019): 3035-3049..
13. Eum, D.,et al. "Voltage decay and redox asymmetry mitigation by reversible cation migration in lithium-rich layered oxide electrodes." *Nature materials* 19.4 (2020): 419-427.
14. Kroll, Jesse H., et al. "The complex chemical effects of COVID-19 shutdowns on air quality." *Nature Chemistry* 12.9 (2020): 777-779.
15. Getahun, et al. "Flood hazard assessment and mapping of flood inundation area of the Awash River Basin in Ethiopia using GIS and HEC-GeoRAS/HEC-RAS model." *Journal of Civil & Environmental Engineering* 5.4 (2015): 1.
16. Segele, et al. "Seasonal-to-interannual variability of Ethiopia/horn of Africa monsoon. Part I: associations of wavelet-filtered large-scale atmospheric circulation and global sea surface temperature." *Journal of Climate* 22.12 (2009): 3396-3421.
17. Taylor, et al. "Summarizing multiple aspects of model performance in a single diagram." *Journal of geophysical research: atmospheres* 106. D7 (2001): 7183-7192.
18. Wilby, et al. "SDSM—a decision support tool for the assessment of regional climate change impacts." *Environmental Modelling & Software* 17.2 (2002): 145-157.
19. Wilby, R. L., and Dawson, C. W. "SDSM 4.2—A decision support tool for the assessment of regional climate change impacts. 2007." (2013).
20. Abebe,et al. "Assessment of Future Climate Change Scenario in Halaba District, Southern Ethiopia." *Atmospheric and Climate Sciences* 12.2 (2022): 283-296.
21. Phuong, et al. "Projections of future climate change in the Vu Gia Thu Bon River Basin, Vietnam by using statistical downscaling model (SDSM)." *Water* 12.3 (2020): 755.
22. Liu, Jiaxu, et al. "Statistical downscaling and projection of future air temperature changes in Yunnan Province, China." *Advances In Meteorology* (2017).
23. Räisänen, et al. "Projections of daily mean temperature variability in the future: cross-validation tests with ENSEMBLES regional climate simulations." *Climate dynamics* 41 (2013): 1553-1568.
24. Wilby, Robert L., et al. "The statistical downscaling model-decision centric (SDSM-DC): conceptual basis and applications." *Climate Research* 61.3 (2014): 259-276.
25. Schoof, et al. "Evaluation of the NCEP–NCAR reanalysis in terms of synopticscale phenomena: a case study from the Midwestern USA." *International Journal of Climatology: A Journal of the Royal Meteorological Society* 23.14 (2003): 1725-1741.
26. Feyissa, et al. "Downscaling of future temperature and precipitation extremes in Addis Ababa under climate change." Climate 6.3 (2018): 58.
27. Choi, Gwangyong, et al. "Changes in means and extreme events of temperature and precipitation in the AsiaPacific Network region, 1955–2007." *International Journal of Climatology: A Journal of the Royal Meteorological Society* 29.13 (2009): 1906-1925.
28. Riahi, Keywan, et al. "RCP-8.5: exploring the consequence of high emission trajectories." *Climatic Change* 109.33 (2011): 10-1007.
29. San José, Roberto, et al. "Impacts of the 4.5 and 8.5 RCP global climate scenarios on urban meteorology and air quality: Application to Madrid, Antwerp, Milan, Helsinki and London." *Journal of Computational and Applied Mathematics* 293 (2016): 192-207..
30. Thomson, Allison M., et al. "RCP4. 5: a pathway for stabilization of radiative forcing by 2100." *Climatic change* 109 (2011): 77-94..
31. Masui, et al. "An emission pathway for stabilization at 6 Wm− 2 radiative forcing." *Climatic change* 109 (2011): 59-76..
32. Van Vuuren , et al. "The representative concentration pathways: an overview." Climatic change 109 (2011): 5-31.
33. Koudahe, K., et al. "Trend analysis in standardized precipitation index and standardized anomaly index in the context of climate change in Southern Togo." *Atmospheric and Climate Sciences* 7.04 (2017): 401.
34. Moss, et al. "Towards new scenarios for analysis of emissions, climate change, impacts, and response strategies". No. PNNL-SA-63186. Pacific Northwest National Lab.(PNNL), Richland, WA (United States), 2008.
35. Moss, R. H. et al., "The next generation of scenarios for climate change research and assessment," *Nature*, vol. 463, no. 7282, pp. 747–756, 2010, doi: 10.1038/nature08823.
36. Ozbuldu, et al. "Evaluating the effect of the statistical downscaling method on monthly precipitation estimates of global climate models." *GLOBAL NEST JOURNAL* 23.2 (2021): 232-240.
37. Najafi, et al. "Uncertainty modeling of statistical downscaling to assess climate change impacts on temperature and precipitation." *Water resources management* 31 (2017): 1843-1858.
38. F. Soil and E. Projects, "Model Calibration, Validation, and Verification Guidance For Soil Enrichment Projects," no. August, 2020.

Cite this article: Abebe, T., et al. Projections of Future Surface Air Temperature and Precipitation for the Middle Awash River Basins in Ethiopia using a Statistical Downscaling Model (SDSM), *J Climatol Weather Forecast*, 2023, 11(1), 001-09.